Vol. 16, pp. 1–8 (2019)
doi: 10.2142/biophysico.16.0_1

Biophysics and Physicobiology

https://www.jstage.jst.go.jp/browse/biophysico/

Regular Article

Millimeter-sized belt-like pattern formation of actin filaments in solution by interacting with surface myosin *in vitro*

Kentaro Ozawa[1], Hirotaka Taomori[1], Masayuki Hoshida[1], Ituki Kunita[2], Sigeru Sakurazawa[3] and Hajime Honda[1]

[1]*Department of Bioengineering, Nagaoka University of Technology, Nagaoka, Niigata 940-2188, Japan*
[2]*Department of Information Engineering, University of the Ryukyus, Nakagami-gun, Okinawa 903-0213, Japan*
[3]*School of System Information Science, Department of Complex and Intelligent Systems, Future University Hakodate, Hakodate, Hokkaido 041-8655, Japan*

Received September 10, 2018; accepted December 14, 2018

The movements of single actin filaments along a myosin-fixed glass surface were observed under a conventional fluorescence microscope. Although random at a low concentration, moving directions of filaments were aligned by the presence of over 1.0 mg/mL of unlabeled filaments. We found that actin filaments when at the intermediate concentrations ranging from 0.1 to 1.0 mg/mL, formed winding belt-like patterns and moved in a two-directional manner along the belts. These patterns were spread over a millimeter range and found to have bulged on the glass in a three-dimensional manner. Filaments did not get closer than about 37.5 nm to each other within each belt-pattern. The average width and the curvature radius of the pattern did not apparently change even when the range of actin concentrations was between 0.05 and 1.0 mg/mL or the sliding velocity between 1.2 and 3.2 μm/sec. However, when the length of filaments was shortened by ultrasonic treatments or the addition of gelsolin molecules, the curvature radius became small from 100 to 60 μm. These results indicate that this belt-forming nature of actin filaments may be due to some inter-filament interactions.

Corresponding author: Hajime Honda, Department of Bioengineering, Nagaoka University of Technology, 1603-1, Kamitomioka Nagaoka, Niigata 940-0213, Japan.
e-mail: hhonda@vos.nagaokaut.ac.jp

Key words: actin filament, motility assay

Actin and its related molecules exist in all known living bodies, maintaining or transforming a cell's shape, or transporting intracellular vesicles. In order to actualize these functions, actin molecules form filaments as a rail to interact with myosin molecules which hydrolyze Mg-ATP to supply energy for generating forces. When actin filaments are functioning, they are usually arranged regularly, such as sarcomeres in muscle cells or a contractile ring during cytoplasmic divisions.

In order to verify the motile activity of actin or myosin molecules, a variety of methods have been developed [1–3]. One of them is the gliding assay of actin filaments which consists of only actin and heavy meromyosin (HMM), the catalytic domain of myosin, which is spread on a glass surface. The sliding motion of each actin filament is initiated by the addition of Mg-ATP and can be observed by fluorescence microscopy. However, the concentration of visible actin filaments must be kept lower than about 1.0 μg/mL to obtain a clearly separated image of each fluorescent filament. This constraint can be overcome by adding unlabeled filaments. This technique enables the observation of not only single

◀ ***Significance*** ▶

Actin filaments slide along myosin molecules on the glass surface. When the concentration of actin filaments was raised to 0.5–1.0 mg/mL, we found that the filaments assembled spontaneously to form a belt-like winding pattern. The pattern formation accompanied by a spontaneous imbalance of concentration in this simple assay system was observed for the first time, indicating that these types of pattern formation may be caused by the intrinsic properties of actin filament even *in vivo*.

filaments but also the self-organization of crowded filaments which has recently been the subject of focus.

In 1997, the helical pattern of taxol-stabilized microtubules driven by multimeric kinesin motors was reported to be self-organized [4,5]. That organization of specific patterns could be formed in the presence of a variety of bundling proteins but those dynamic phenomena could not be predicted by theoretical models at that time [6]. Another aspect of actin filaments was reported by Brestschneider, T., *et al.* [7]. They suggested that the assemblage of actin filaments occurred as a wave-like motion and that the recruitment of proteins from the solution-pool might be important for this pattern formation. These two-dimensionally crowded conditions of actin filaments were further tested in a flow chamber by Schaller, V., *et al.* [8]. They showed a polar pattern of formation in addition to wave-like patterns. They further noted that weak interactions and local alignment should be essential for the formation of these patterns. At almost the same time, Butt, T., *et al.* also demonstrated the alignment of actin filaments with unlabeled actin filaments in solution [9]. They claimed that the shape of the alignment depended on both the length and density of actin filaments and that these patterns changed at a time scale of several seconds. This phenomenon was theoretically analyzed by Chaté, H., *et al.* [6], who claimed that the inelastic collisions of filaments caused their nematic alignment. Shortly thereafter, the spontaneous formation of a large-scale vortex of microtubules driven by dynein and its mathematical model, including nematic alignment due to the collision of microtubules, were demonstrated in 2012 [10]. Another collective motion of microtubules driven by a cluster of two kinesin molecules in the presence of polyethylene glycol was also demonstrated by Sanchez, T., *et al.* [11].

In any of the above cases, both the recruitment, i.e., landing of filaments from solution onto the motor-coated surface, and the nematic interactions between them, may play an essential role in these phenomena. From this point of view, we tried to simultaneously introduce unlabeled actin filaments mixed together with a slight amount of labeled filaments as a reporter onto a myosin-coated glass surface. This system may reveal not only the process of recruitment of filaments from solution but also the nematic collision of filaments because myosin-driven actin filaments purportedly do not collide with each other [11].

As a result, belt-like patterns that are millimeters in size formed under conventional assay conditions when labeled and unlabeled actin filaments were mixed at a 1:1000 ratio on the glass surface and in solution. The size, regularity and mechanism of formation were characterized. We succeeded to quantitatively evaluate the amount and rate of recruitment of filaments and found that the direct collision of filaments may not always be necessary for their collective motion. These results suggest that these types of patterns of formation should be caused by the intrinsic and specific nature of actin filaments.

Materials and Methods

Proteins and reagents

Actin molecules were prepared [12] from the acetone powder of chicken tenderloin muscle [13], with slight modifications. Myosin molecules were prepared from rabbit skeletal muscle [14] followed by HMM preparation [15]. Concentrations were determined by differences in extinction coefficients between 310 and 290 nm, namely 0.62 ($\varepsilon_{290}-\varepsilon_{310}=0.62$) for actin solution and $\varepsilon_{280}=0.60$ for HMM.

ATP, gelsolin from bovine plasma, phalloidin and rhodamine-labeled phalloidin (Rho-Ph) were purchased from Sigma-Aldrich Co. LLC. Trimethylsilyl chloride (TMCS) was purchased from Shin-Etsu Chemical Co., Ltd. All other reagents were of special reagent grade from FUJIFILM Wako Pure Chemical Corp.

Specimens and microscopic chamber

1) For each chamber

Glass covers of two sizes, 18×18 mm and 25×50 mm (Matsunami, Neo cover glass No. 1), were cleaned by incubating them in piranha solution, i.e., a 1:1 (v/v) mixture of sulfuric acid (H_2SO_4) and hydrogen peroxide (H_2O_2), for 30 min. After washing them with pure water, glass covers were dipped in 5% TMCS-ethanol solution overnight, washed twice each with absolute ethanol and pure water, then dried in clean air before use.

A square (18×18) glass was mounted on the center of a rectangular (25×50) glass by two pieces of double-sided sticky tape, which was 0.15 mm thick (Nichiban, Nice-tack HW-K15). Tape, which was placed in parallel on the glass slide, was separated by about 5.0 mm, and the size of each chamber was 18×5×0.15 mm with both sides open.

2) Specimens

Unlabeled actin (2.0 mg/mL) was polymerized in 0.1 M KCl with buffer 1 (2.0 mM Tris-HCl (pH=8.4), 2.0 mM $MgCl_2$, 0.5 mM ATP and 1.0 mM DTT) at 4°C overnight. Rho-Ph was labeled by incubating 0.1 mg/mL actin, 3.25 μg/mL Rho-Ph and 25 mM KCl in buffer 1 at 4°C overnight.

The protein solutions were perfused from one side of the chamber, in this order: (1) buffer 2 (25 mM KCl, 25 mM imidazole-HCl (pH=7.4), 4.0 mM $MgCl_2$, 2.0 mM ATP and 100 mM DTT), (2) 0.1 mM HMM in buffer 2 followed by 2 min incubation, (3) 1.0 μg/mL unlabeled actin in buffer 2, and (4) 1.0 μg/mL Rho-Ph-labeled actin with the required concentrations of unlabeled actin filaments. All procedures were performed in an air-conditioned room at 25°C with relative humidity below 50%.

Ultrasonication with 20 kHz was performed on ice for repeated cycles of 0.5 sec of a 0.5 W dose at 0.5 sec intervals by an ultrasonic homogenizer (Smurt NR-50M). The fragmented filaments were subjected to the pattern-formation experiments within 5 min.

Observation

The chambers were mounted on a fluorescence microscope (Nikon, Eclipse TE-2000U) with a 60× objective (Nikon, Plan Apo VC 60x (NA = 1.40)). Images were recorded in two ways depending on the temporal and spatial requirements. The first method used an EM-CCD TV camera (Hitachi Kokusai Electric, KP-E500) attached to the side-port of the microscope while the second method used a conventional digital camera (Canon, EOS Kiss X7i) attached to the front port of the microscope. TV images were recorded on a PC by an image grabber board (The Imaging Source, DFG/SVI PCI grabber) and controller (The Imaging Source, IC Capture) in an uncompressed AVI format (UYVY, 640 × 480 pixels, 30 fps). Still images were recorded in TIFF format (0.5 sec exposure, ISO=12800, 3456 × 3456 pixels). A wide-angle image was obtained by an All-in-one Fluorescence Microscope (Keyence, BZ-X700). Images were analyzed on a PC by Image-J software.

Image analysis

Sliding speed and the direction of filaments were calculated from the velocity vector during about 0.5 sec, i.e., 15 frames. The number of filaments attaching to the glass slide surface was counted within 10×10 μm in a given snapshot. The width and curvature radius of the belt-like-pattern were calculated by Image-J software with original add-ons as follows: (1) experimental noise of pictures was reduced by a band-pass filter of spatial frequency, (2) the image was binarized in order to calculate their width and (3) was skeletonized to obtain curvatures. The width of a belt-like pattern at a specific point was calculated from the diameter of the inscribed circle centered on a skeletonized line. Curvature radius was calculated from the circle that passes three points along the skeletonized line with 10 μm between each point. Only when the belt-like pattern continued for more than 20 μm was it measured. Inter-filament distances were estimated by measuring the distances of labeled filaments and estimating the actual distances by assuming that the physical property of all filaments was the same. The accuracy of the data was shown with 95% confidence intervals obtained from 50 measurements.

Estimation of inter-filament distances

The depth of focus (DOF) was calculated by Berek's equation [16]:

$$\mathrm{DOF} = \omega \times 250{,}000/(\mathrm{NA} \times \mathrm{M}) + \lambda/(2 \times \mathrm{NA}^2)$$

where ω is the resolving power of eyes = 0.0014, NA is the numerical aperture on the objective lens = 1.4, M is total magnification=200, λ is the wavelength of the light used = about 600 nm. According to the equation, the DOF of our system was 1.4 μm. In this context, when we counted 10 filaments within a 10 μm (width) × 1.4 μm (depth) cross-section, the average distance of filaments was calculated to be about 37.5 nm.

Results

The emergence of belt-like patterns

When 0.5 mg/mL of F-actin solution with Mg-ATP was initially perfused into the microscopic chamber, random touching down of visible filaments was observed, and the direction of the movement was random. However, as the number of visible filaments increased, the directions of moving filaments transformed from random to aligned, as shown in Figure 1 panels (a) to (d). Several minutes later, the distribution of filaments was found to be biased, forming belt-like patterns as shown in Figure 1 panel (e). Panel (f) shows a close-up of the square area in panel (e) where low and high-density areas were observed near the boundary of a belt. This figure indicates that the intensity from the inside of the belt-pattern area was higher than that from outside.

In order to quantitatively evaluate the filament number during this process the number of actin filaments within a 20 × 20 mm^2 area was counted as shown in panel (a) of Figure 1. The number appeared to increase in two steps i.e., the first step occurred about 2 min after the reaction started and the second started about 3 min after. The first increase is thought to be caused by the touching down of filaments on the glass surface from solution. However, the second increase may be caused by the gathering of filaments to form a belt-pattern as can be observed in the right half of panel (f). Such a stepwise increase was observed over a wide range and the belt-like pattern spread to the entire specimen as can be shown in Figure 3.

The patterns emerged about 5 min after the reaction started and found to be transformed continuously for several minutes. A typical temporal change in pattern after 5 min is shown in Figure 4. However, the shape did not change about 30 min after the reaction started until the sliding motion ceased by exhaustion of Mg-ATP in solution. When the pattern was disrupted by another flow of actin filaments solution with Mg-ATP, a similar but not identical pattern was formed. From the result, the patterns were thought to be formed independently of the HMM distribution over the glass.

Inter-filament distance within a belt and characterization of the shape

In order to estimate the inter-filament distances within a belt, we counted the number of filaments within a focal plane at 30 min after the reaction started. The method to estimate actual distances will be explained in the discussion section. As the total protein concentration increased, distances decreased and reached a minimum of about 37.5 nm as shown in Figure 5. Hereafter, all data has a 95% confidence interval.

Effects of sliding velocity

As the pattern appears to consist of jointed curved-belts, we attempted to quantitatively characterize it by measuring

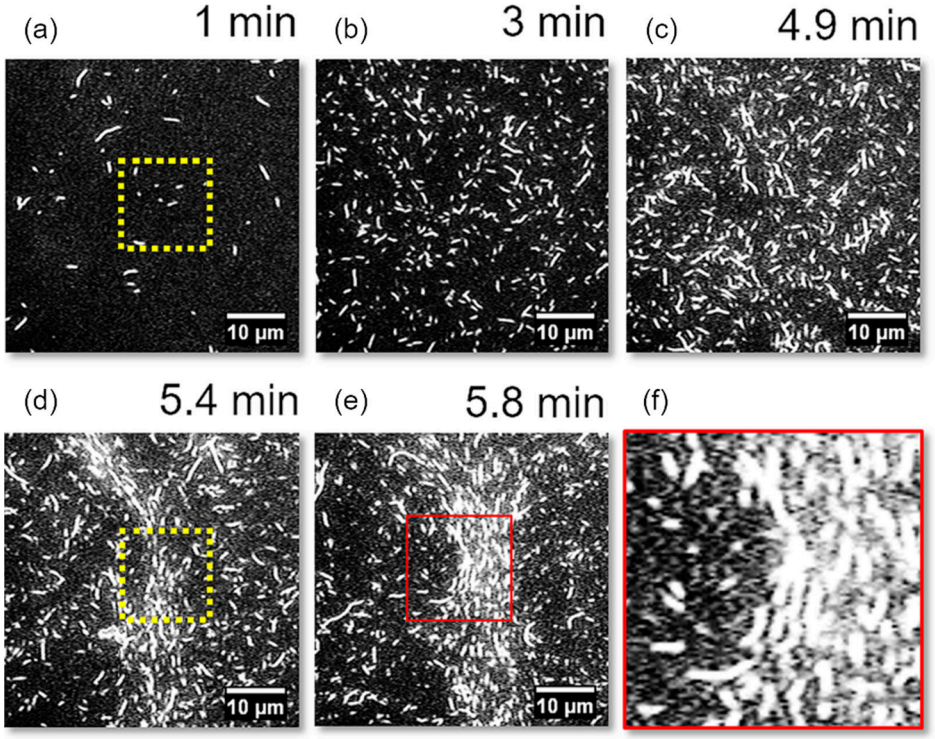

Figure 1 Typical process of a local band-pattern formation. Sequential photographs (a)–(e) show a time-dependent assembly of actin filaments at 1.0, 3.0, 4.9, 5.4, and 5.8 min, respectively after starting the sliding motion. The concentration of actin was 0.5 mg/mL. The square-box in panel (a) indicates the area used to count the number of filaments in Figure 2. Scale bar: 10 μm. Panel (f) shows a close-up of the red square area in (e).

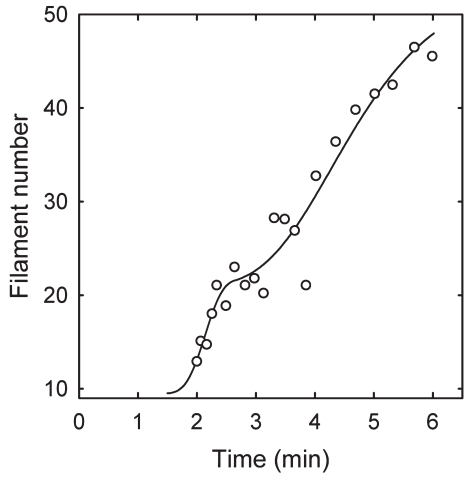

Figure 2 Changes in the number of actin filaments. The number of filaments was measured in the areas indicated in Figure 1(a). The curved line indicating stepwise increase was drawn by hand as an auxiliary.

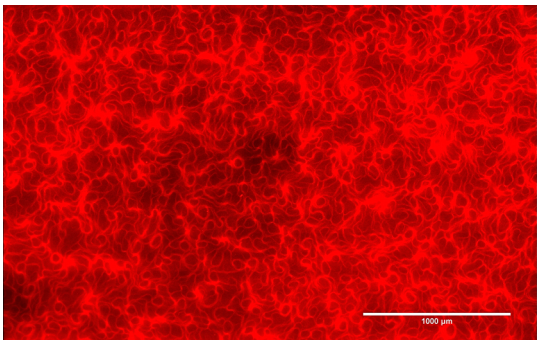

Figure 3 Large-scale formation of a band pattern. Photograph of a band pattern observed in a wide range taken 30 min after initiating the sliding motion. The concentration of actin was 100 μg/mL. The photo was taken near the center of the chamber. Video movies obtained from the EMM-CCD camera were superimposed on the color still images of the same position of a specimen.

the curvature radius and the width of the belt 30 min after the reaction started. Fifty intervals within a belt sandwiched between two branching points were measured for each experiment.

In order to examine the effects of sliding velocity on the shape of patterns, the concentration of Mg-ATP was lowered in the ATP regenerating system. The results are shown in Figure 6 where sliding velocity was plotted against Mg-ATP concentration. Sliding velocity did not appear to change the shape of patterns. From these results, we have tried to check the effects of the average length of filaments.

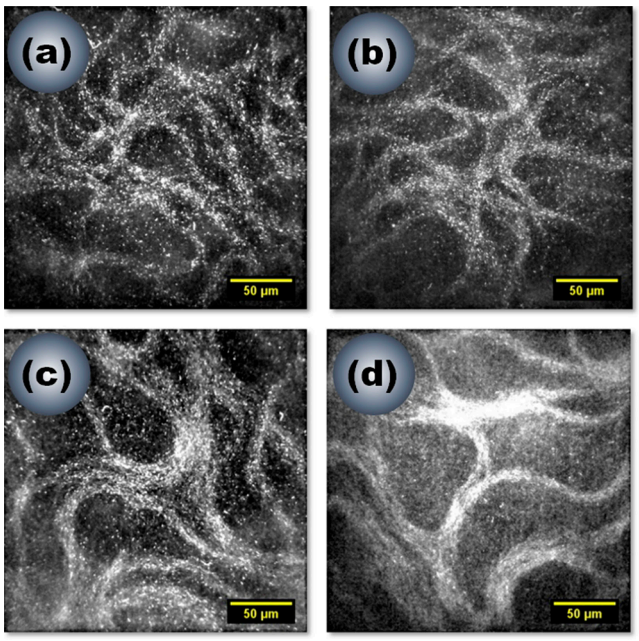

Figure 4 Time-dependent changes in belt-like patterns. Photos in panels (a)–(d) were taken 10, 20 30, and 70 sec, respectively after 5 min had elapsed since the reaction started. The concentration of actin was 0.5 mg/mL. Scale bars: 50 μm.

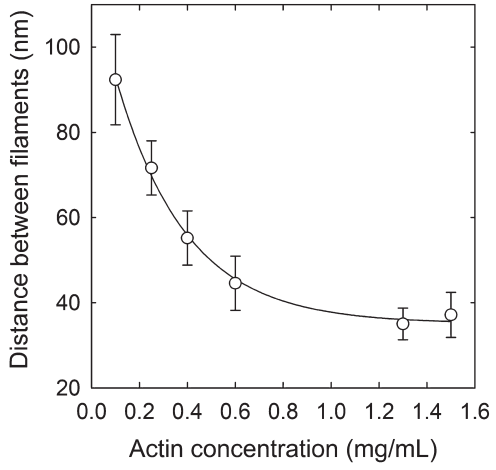

Figure 5 Effects of actin concentration on inter-filament distances within belt-like patterns. Inter-filament distances were estimated against the concentration of actin. The method of estimation was elaborated in the discussion section. Error bars represent half of the standard deviation. n=50.

Effects on average filament length

To investigate the effects of filament length on the shape of patterns, two methods were adopted: one is the application of ultrasonication while the other is the addition of gelsolin molecules. In the first method, the curvature radius (a) and width of the belts (b) with different doses of ultrasound were plotted (open symbols in Fig. 7). Gelsolin molecules were added at a molar ratio of 1:800, 1:400 and 1:300

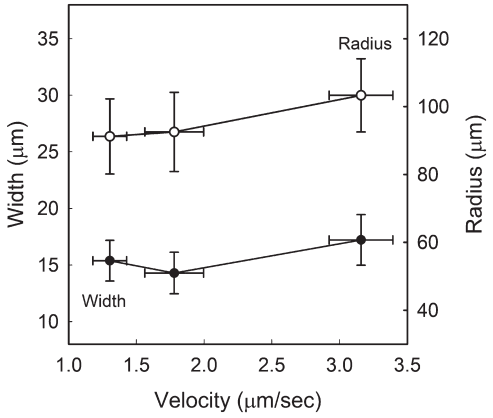

Figure 6 Effect of sliding velocities on the shape of belt-like patterns. The concentration of Mg-ATP ranged between 0.2 and 2.0 mM to vary the sliding velocity. Actin concentration was 0.1 mg/mL. The curvature radius and width were plotted as open and filled circles, respectively. In order to avoid exhaustion of Mg-ATP, an ATP-regenerating enzyme-system [22] was adopted. Error bars represent half of the standard deviation. n=50.

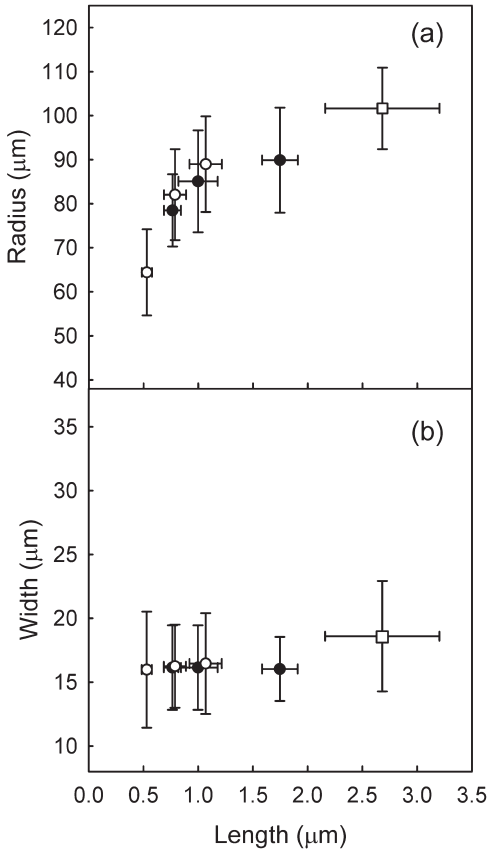

Figure 7 Effect of filament length on the shape of belt-like patterns. The relationship is shown between average length and curvature radius in (a) and curvature width in (b). Data from the ultrasonication treatment and from the addition of gelsolin were plotted as open and filled circles, respectively. Error bars represent half of the standard deviation. n=50. Data indicated at an average length of 2.6 μm were obtained from samples without either treatment.

to actin molecules in the presence of 10 mM EGTA. These results have been plotted in Figure 7 as filled symbols. Curvature clearly increased as average length increased but not the width.

Discussion

Characterization of the belt-like pattern formation

Recently, many types of pattern formation in actin solution systems have been reported. They may be classified into three types. First, an extremely high concentration of actin filaments, without HMM, forming liquid crystalline-like domains in solution [17] or cable-stitched winding bundles when filaments were further concentrated [18]. In the second type [8,9], both labeled and unlabeled filaments co-localized and moved along the HMM coated glass surface to assess the crowded conditions but no floating filaments were present in solution. In the third type [19], in addition to the former compositions of filaments, unlabeled, without labeled, filaments were added to the solution. In the third type, Taking these three types of pattern formation into consideration, in the present report, we introduced both labeled and unlabeled filaments into a solution with Mg-ATP from the beginning of experiments. Using this system, we successfully observed the behavior of filaments in all processes related to pattern formation at intermediate concentrations.

Two-step increase in filament number

Figure 2 shows an increase in the number of actin filaments within a certain area over time. This increase apparently occurred in two steps, one from 2 to 2.5 min and another from 3.0 to 6.0 min after initiating the sliding movement. The supplementary line simply indicates our interpretation as described above. From the microscopic observations (Fig. 1), the first increase may have occurred by the recruitments of filaments to the glass surface from solution. However, the second increase was undoubtedly caused by the assembly of filaments that cause the formation of a belt-like pattern. It may seem rather strange that moving actin filaments interact directly with other filaments in solution. However, there are several reports that support the long-distance interaction of the actomyosin system [20,21]. So, this assembly of the filament may have caused by some attractive forces between actin filaments. The first increase must correspond to the simple addition of new filaments from solution but the second increase seems to be caused by the association of external filaments in the measured area. The second increase may accelerate the further addition of filaments from the solution. In this sense, filaments may interact with other filaments by some viscous interaction such as viscous coupling.

Determining factors of large curvature radius

Actin filaments are known to move in a helical manner, so a force may cause winding of their moving path. However, only the pitch of an actin filament is too small to explain the curvature radius of belt-like patterns. Tight coupling between the helix and the direction of their movement should reduce the curvature to less than 1.0 μm. We took into account the fact that the filament could not approach the neighboring filament less than about 37 nm, as shown in Figure 5, allowing the water molecules surrounding a filament to mediate the viscoelastic interaction between filaments and form apparently large bundles of filaments with loose semi-flexibility. Similar bundles were observed in a high concentration of the F-actin solution. Apparent bundles composed of many filaments with a variety of lengths might receive energy from ATP hydrolyzed by surface HMM molecules, forming a slight angle to the filament axis. This hypothesis could explain the smaller radius at a shorter filament length because the sum of shorter filaments should possess a less elastic property.

Relation of the pattern formation with volume exclusion effects

The formation of a bundle-like pattern is sometimes caused by volume exclusion effects such as the addition of polyethylene glycol or methylcellulose [22]. In the above case, however, the bundle was observed to be tighter and more rigid relative to the patterns reported here. When a slight amount of methylcellulose (0.001%) was added, the belt-like patterns in this report did not form. These observations indicate that our observed belt-like patterns are likely not formed by simple volume exclusion effects. However, the curvature radius and the width of the texture patterns observed during this process, especially before drying up, seems to be similar to the one reported here. These observation might suggest other types of inter-filament interactions.

Effects of phalloidin and rhodamine dye on pattern formation

It was well known that polymers containing hydrophobic groups are tend to self-associated to form macroscopic structures [23]. In this context, we attempted to check whether rhodamine-phalloidin containing a hydrophobic group might have any effect on the pattern formations. We performed the same pattern-formation experiments without phalloidin molecules at the same experimental solutions. After incubating samples until all Mg-ATP had been exhausted, buffers containing rhodamine-phalloidin were perfused without ATP to stain all the actin filaments in the specimen. The results are shown in Figure 8. As essentially the same patterns could be observed, we concluded that this pattern of formation was not caused by the presence of phalloidin-rhodamine.

Possible redistribution of HMM molecules on the glass surface

To avoid the possibility that HMM molecules move along the glass surface to assemble along the belt-pattern, we tested the reformation of the pattern. After formation of the belt-like patterns, newly prepared F-actin solution with

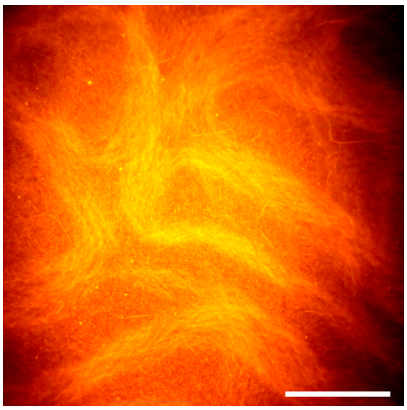

Figure 8 Phalloidin-rhodamine–stained actin filaments. Actin filaments covering the glass surface were stained after exhausting ATP. All the filaments in the specimen with an original concentration of actin of 50 µg/mL are visualized. Scale bar: 50 µm.

Mg-ATP was reintroduced into the chamber. Although the patterns were destroyed by injection flow, other patterns with different shapes formed after 30 min. To explain this phenomenon, it seems natural to consider that the patterns were formed by the intrinsic property of actin filaments rather than the redistribution of HMM molecules.

Evaluation of inter-filament distances

Inter-filament distances, as shown in Figure 3, were calculated provided that invisible filaments relative to visible filaments were present at a ratio of 1:1000. Initial estimates of the distance took into account that all filaments were arranged on a planar, two-dimensional glass surface. In Figure 1, the visible number of filaments within a cross-sectional line of a single belt, about 10 µm long, was estimated at about 10. In this condition, the inter-filament distance would become 1.0 nm, as shown in the upper panel of Figure 9. Considering that the size of an actin filament is about 6 nm, this hypothesis must be incorrect. As a result, filaments should be considered to be three-dimensionally arranged to some extent. This hypothesis is also supported by the observation that the background brightness of inter-filament images within a belt-pattern, as shown in a close-up image in panel (f) of Figure 1, was brighter than external to the belt. However, there are 10 fluorescent filaments in the area of the cross section of 10 µm (width) × 1.4 µm (depth), so the number of actin filament is 10,000 (i.e. 10 (labeled) × 1000 (unlabeled)). Therefore, the cross-sectional area per actin filament is 1400 nm^2, and the distance between actin filaments is 37.5 nm which is the square root of 1,400 nm, as shown in the lower panel of Figure 9. Why a three-dimensional belt forms remains unclear. One possibility is that this distance might originate from the viscous interactions of water molecules between filaments [24].

Belt-like pattern and the nature of actin filament

This pattern was formed very easily and reproducible in our experiments. Why then was it not reported in the preceding reports? As this pattern hardly formed on the collodion-coated surface, the reason may be related to the surface treatment. We treated the glass surface with TMCS for a long period of time, i.e. overnight, with a thorough wash with absolute ethanol. This process may allow the formation of a planer arrangement of hydrophobic silane groups. This may suggest that the complete planer surface

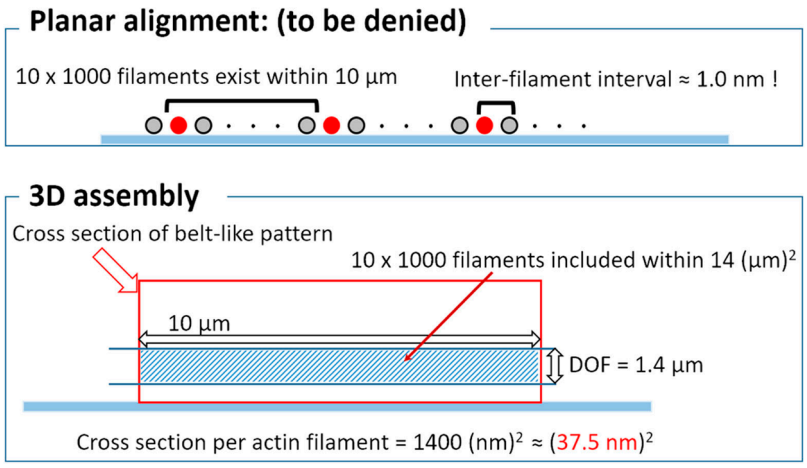

Figure 9 Schematic drawing of the supposed cross-section of a belt-like pattern. Two hypotheses of the packing-arrangements of filaments within a belt area of the pattern were compared. In the upper panel, filaments were assumed to be arranged in a plane along the myosin-coated surface. Red and gray circles indicate the cross section of labeled (visible) and unlabeled (invisible) filaments, respectively. In this case, the inter-filament interval was calculated to be 1.0 nm. In the lower panel, filaments were assumed to be piled up in a 3D manner. The blue-hatched area indicates the cross section of the observed pattern, a rectangle with sides to 10 µm of measurement distance and 1.4 µm of the depth of field of microscope. Within this area of 10×4 µm^2, 10×1000 filaments were assumed to exist. Thus, the cross section per actin filament was calculated to be (37.4 nm)^2.

allowed to emerge the intrinsic nature of actin filament.

We have found that the molecular-dispersed actin filament formed belt-like patterns, including the non-uniform distribution of filaments [25], so it might be worth considering the pattern formations [26,27] of a living body.

Conflicts of Interest

All authors declare that they have no conflicts of interest.

Ethics

This study was reviewed and approved by the Nagaoka University of Technology Research Ethics Committee.

Author Contribution

K. O., H. T., and M. H. performed the experiments. I. K. and S. S. analyze the pattern shape. H. H. directed the entire project and wrote the manuscript.

References

[1] Kron, S. J. & Spudich, J. A. Fluorescent actin filaments move on myosin fixed to a glass surface. *Proc. Natl. Acad. Sci. USA* **83**, 6272–6276 (1986).
[2] Honda, H., Nagashima, H. & Asakura, S. Directional movement of F-actin in vitro. *J. Mol. Biol.* **191**, 131–133 (1986).
[3] Holzbaur, E. L. & Goldman, Y. E. Coordination of molecular motors: from *in vitro* assays to intracellular dynamics. *Curr. Opin. Cell Biol.* **22**, 4–13 (2010).
[4] Ndlec, F. J., Surrey, T., Maggs, A. C. & Leibler, S. Self-organization of microtubules and motors. *Nature* **389**, 305–308 (1997).
[5] Surrey, T., Nédélec, F., Leibler, S. & Karsenti, E. Physical properties determining self-organization of motors and microtubules. *Science* **292**, 1167–1171 (2001).
[6] Chaté, H., Ginelli, F., Grégoire, G. & Raynaud, F. Collective motion of self-propelled particles interacting without cohesion. *Phys. Rev. E Stat. Nonlin. Soft Matter Phys.* **77**, 046113 (2008).
[7] Bretschneider, T., Anderson, K., Ecke, M., Müller-Taubenberger, A., Schroth-Diez, B., Ishikawa-Ankerhold, H. C., *et al.* The three-dimensional dynamics of actin waves, a model of cytoskeletal self-organization. *Biophys. J.* **96**, 2888–2900 (2009).
[8] Schaller, V., Weber, C., Semmrich, C., Frey, E. & Bausch, A. R. Polar patterns of driven filaments. *Nature* **467**, 73–77 (2010).
[9] Butt, T., Mufti, T., Humayun, A., Rosenthal, P. B., Khan, S., Khan, S., *et al.* Myosin motors drive long range alignment of actin filaments. *J. Biol. Chem.* **285**, 4964–4974 (2010).
[10] Sumino, Y., Nagai, K. H., Shitaka, Y., Tanaka, D., Yoshikawa, K., Chaté, H., *et al.* Large-scale vortex lattice emerging from collectively moving microtubules. *Nature* **483**, 448–452 (2012).
[11] Sanchez, T., Chen, D. T., DeCamp, S. J., Heymann, M. & Dogic, Z. Spontaneous motion in hierarchically assembled active matter. *Nature* **491**, 431–434 (2012).
[12] Spudich, J. A. & Watt, S. The regulation of rabbit skeletal muscle contraction I. Biochemical studies of the interaction of the tropomyosin-troponin complex with actin and the proteolytic fragments of myosin. *J. Biol. Chem.* **246**, 4866–4871 (1971).
[13] Pardee, J. D. & Aspudich, J. [18] Purification of muscle actin. in *Methods in Enzymology* vol. 85, pp. 164–181 (Elsevier, 1982).
[14] Ebashi, S. & Ebashi, F. A new protein component participating in the superprecipitation of myosin B. *J. Biochem.* **55**, 604–613 (1964).
[15] Okamoto, Y. & Sekine, T. A streamlined method of subfragment one preparation from myosin. *J. Biochem.* **98**, 1143–1145 (1985).
[16] Chamot, E. M. & Mason, C. W. Handbook of chemical microscopy. (John Wiley And Sons, Newn York, 1938).
[17] Furukawa, R., Kundra, R. & Fechheimer, M. Formation of liquid crystals from actin filaments. *Biochemistry* **32**, 12346–12352 (1993).
[18] Honda, H. & Ishiwata, S. Two-dimensional periodic texture of actin filaments formed upon drying. *Biophysics* **7**, 11–19 (2011).
[19] Schaller, V., Weber, C., Frey, E. & Bausch, A. R. Polar pattern formation: hydrodynamic coupling of driven filaments. *Soft Matter* **7**, 3213 (2011).
[20] Hatori, K., Honda, H. & Matsuno, K. ATP-dependent fluctuations of single actin filaments in vitro. *Biophys. Chem.* **58**, 267–272 (1996).
[21] Kunita, I., Sakurazawa, S. & Honda, H. Up-and-down movement of a sliding actin filament in the *in vitro* motility assay. *BioSystems* **103**, 79–84 (2011).
[22] Iwase, T., Sasaki, Y. & Hatori, K. Alignment of actin filament streams driven by myosin motors in crowded environments. *Biochim. Biophys. Acta Gen. Subj.* **1861**, 2717–2725 (2017).
[23] Yang, X., Liu, J., Li, P. & Liu, C. Self-assembly properties of hydrophobically associating perfluorinated polyacrylamide in dilute and semi-dilute solutions. *J. Poly. Res.* **22**, 103 (2015).
[24] Suzuki, M., Kabir, S. R., Siddique, M. S., Nazia, U. S., Miyazaki, T. & Kodama, T. Myosin-induced volume increase of the hyper-mobile water surrounding actin filaments. *Biochem. Biophys. Res. Commun.* **322**, 340–346 (2004).
[25] Wang, S. & Wolynes, P. G. On the spontaneous collective motion of active matter. *Proc. Natl. Acad. Sci. USA* **108**, 15184–15189 (2011).
[26] Kamasaki, T., Osumi, M. & Mabuchi, I. Three-dimensional arrangement of F-actin in the contractile ring of fission yeast. *J. Cell Biol.* **178**, 765–771 (2007).
[27] Sanger, J. W. Changing patterns of actin localization during cell division. *Proc. Natl. Acad. Sci. USA* **72**, 1913–1916 (1975).